The Astrophysical Journal, 568:779–790, 2002 April 1

ON THE THERMONUCLEAR RUNAWAY IN TYPE Ia SUPERNOVAE: HOW TO RUN AWAY?

P. Höflich[1] and J. Stein[2]

Received 2001 April 12; accepted 2001 December 5

ABSTRACT

Type Ia supernovae (SNe Ia) are thought to be thermonuclear explosions of massive white dwarfs (WDs). We present the first study of multidimensional effects during the final hours prior to the thermonuclear runaway that leads to the explosion. The calculations utilize an implicit, two-dimensional hydrodynamic code. Mixing and the ignition process are studied in detail. We find that the initial chemical structure of the WD is changed, but the material is not fully homogenized. In particular, the exploding WD sustains a central region with a low C/O ratio. This implies that the explosive nuclear burning will begin in a partially carbon-depleted environment. The thermonuclear runaway happens in a well-defined region close to the center. It is induced by compressional heat when matter is brought inward by convective flows. We find no evidence for multiple spot or strong off-center ignition. Convective velocities in the WD are on the order of 100 km s^{-1}, which is well above the effective burning speeds in SNe Ia previously expected right after the runaway. In our calculations, the ignition occurs near the center. Then, for ≈ 0.5–1 s, the speed of the burning front will neither be determined by the laminar speed nor the Rayleigh-Taylor instabilities but by convective flows produced prior to the runaway. The consequences are discussed for our understanding of the detailed physics of the flame propagation, the deflagration to detonation transition, and the nucleosynthesis in the central layers. Our results strongly suggest the preconditioning of the progenitor as a key factor for our understanding of the diversity in SNe Ia.

Subject headings: hydrodynamics — methods: numerical — supernovae: general — turbulence — white dwarfs

On-line material: color figures

1. INTRODUCTION

Type Ia supernovae (SNe Ia) are among the most spectacular events because they reach the same brightness as an entire galaxy. This makes them good candidates to determine extragalactic distances and to measure the basic cosmological parameters. Moreover, they are thought to be the major contributors to the chemical enrichment of the interstellar matter with heavy elements. Energy injection by supernovae into the interstellar medium, triggered star formation, and feedback in galaxy formation are regarded as key to our understanding of the formation and evolution of galaxies.

There is general agreement that SNe Ia result from some process of combustion of a degenerate C/O white dwarf (WD; Hoyle & Fowler 1960). Within this general picture, three classes of models have been considered:

1. An explosion of a C/O WD, with mass close to the Chandrasekhar mass, which accretes mass through Roche lobe overflow from an evolved companion star (Whelan & Iben 1973). The explosion is then triggered by compressional heating near the WD center.
2. An explosion of a rotating configuration formed from the merging of two low-mass WDs caused by the loss of angular momentum owing to gravitational radiation (Kenyon & Webbink 1984; Iben & Tutukov 1984; Paczyński 1985).
3. Explosion of a low-mass C/O WD triggered by the detonation of a helium layer (Sugimoto & Nomoto 1980; Woosley, Weaver, & Taam 1980; Woosley & Weaver 1984).

Only the first two models appear to be viable. The third, the sub-Chandrasekhar WD model, has been ruled out on the basis of predicted light curves and spectra (Höflich et al. 1996b; Nugent et al. 1997).

For the identification of the most common scenario, the main problem is related to the insensitivity of the WD structure to the progenitor star and system. However, the last decade has witnessed an explosive growth of high-quality data and advances in the models for supernovae that opened up new opportunities to constrain the physics of supernovae. For the first time, a direct connection with the progenitors seems to be within reach. In particular, there is mounting evidence for a connection between the properties of the progenitor, and the physics of the explosion.

The explosion of a WD with $M_{\rm Ch}$ is the most likely candidate for the majority of "normal" SNe Ia. In particular, delayed detonation (DD) models (Khokhlov 1991; Woosley & Weaver 1994; Yamaoka et al. 1992) have been found to reproduce the majority of optical and infrared light curves and spectra of SNe Ia reasonably well (Höflich 1995; Höflich & Khokhlov 1996; Fisher et al. 1998; Nugent et al. 1997; Wheeler et al. 1998; Lentz et al. 2000; Gerardy et al. 2002). We note that detailed analyses of observed spectra and light curves indicate that mergers and deflagration models such as W7 may contribute to the supernova population (Harkness 1987; Höflich & Khokhlov 1996; Hatano et al. 2000). The evidence against pure deflagration models for the majority of SNe Ia includes infrared spectra that show signs of explosive carbon burning at high expansion velocities (e.g., Wheeler et al. 1998), recent calculations for

[1] Department of Astronomy, University of Texas, Austin, Texas; pah@hej1.as.utexas.edu.
[2] Racah Institute of Physics, The Hebrew University, Jerusalem, Israel; yossi@phys.huji.ac.il.

three-dimensional deflagration fronts by Khokhlov (2002) that predict the presence of unburned and partially burned material down to the central regions, and a large amount of unburned material at the outer layers. Mergers are beyond the scope of this paper, but pure deflagration models will be mentioned where appropriate.

The DD model assumes that burning starts as subsonic deflagration and then turns to a supersonic, detonative mode of burning. The amount of ^{56}Ni depends primarily on $\rho_{\rm tr}$ (Höflich 1995; Höflich, Khokhlov, & Wheeler 1995; Iwamoto et al. 1999), and to a much lesser extent on the deflagration speed, and the initial central density and initial chemical composition (ratio of carbon to oxygen) of the WD. In DDs, almost the entire WD is burned; i.e., the total production of nuclear energy is almost constant. This and the dominance of $\rho_{\rm tr}$ for the ^{56}Ni production are the basis of why, to first approximation, SNe Ia appear to be a one-parameter family. The observed $M(\Delta M_{15})$ can be well understood as an opacity effect, namely, the dropping opacity at low temperatures (Höflich et al. 1996a and references therein; Mazzali et al. 2001). Nonetheless, variations of the other parameters lead to some deviation from a one-parameter $M(\Delta M_{15})$ relation with a spread of 0.5 mag (Höflich et al. 1996a). Empirically, the $M(\Delta M_{15})$ has been well established with a rather small statistical error σ (0.12 mag: Riess et al. 1996; 0.16 mag: Schmidt et al. 1998; 0.14 mag: Phillips et al. 1999; 0.16 mag: Riess et al. 1999; 0.17 mag: Perlmutter et al. 1999). This may imply a correlation between free model parameters, namely, the properties of the burning front, the main-sequence mass of the progenitor $M_{\rm MS}$, and the central density of the WD at the time of the explosion.

Recent studies have shown that the chemical structure of the WD will affect the light curves and spectra. The properties of the progenitors must be taken into account to determine cosmological parameters or the cosmological equation of state. In particular, the mean C/O ratio of the exploding WD has been identified as one of the key factors (Höflich, Wheeler, & Thielemann 1998; Hoflich et al. 2000; Umeda & Nomoto 1999; Dominguez, Höflich, & Straniero 2001). From stellar evolution, the WD can be expected to consist of a carbon-depleted central region produced during the convective, central He burning. The central region is surrounded by layers with C/O $\approx$ 1 originating from the He shell burning in the star and from the accretion phase. The size of the carbon-depleted region ranges from 0.1 to about 0.8 $M_\odot$ depending on $M_{\rm MS}$. At the time of the explosion, the C/O WD should show a distinct C and O profile, These dependencies may suggest that the preconditioning of the WD may be key for our understanding of the diversity of supernovae (Höflich et al. 1996a, 1996b). In addition, Arnett & Livne (1994) suggested that the initial velocity fields in the WD prior to the explosion might influence the flame propagation.

The propagation of a detonation front is well understood, but the description of the deflagration front and the deflagration to detonation transition (DDT) pose problems. On a microscopic scale, a deflagration propagates owing to heat conduction by electrons. Although the laminar flame speed in SNe Ia is well known, the front has been found to be Rayleigh-Taylor (RT) unstable, increasing the effective speed of the burning front (Nomoto, Sugimoto, & Neo 1976). More recently, significant progress has been made toward a better understanding of the physics of flames. Starting from static WDs, hydrodynamic calculations of the deflagration fronts have been performed in two dimensions (Niemeyer & Hillebrandt 1995; Reinecke et al. 1999; Lieswski et al. 2000) and three dimensions (e.g., Livne 1993; Khokhlov 1995, 2002). It has been demonstrated that RT instabilities govern the morphology of the burning front in the regime of linear instabilities, i.e., as long as perturbations remain small. During the first second after the runaway, the increase of the flame surface owing to RT remains small, and the effective burning speed is close to the laminar speed ($\approx$50 km s^{-1}) if the ignition occurs close to the center. Khokhlov (2000) also shows that the effective burning speed is very sensitive to the energy release by the fuel, i.e., the local C/O ratio. Therefore, the actual flame propagation will depend on the detailed chemical structure of the progenitor. Niemeyer, Hillebrandt, & Woosley (1996) studied the effect of off-center ignition and demonstrated that multiple spot ignition with significant separation ($\approx 50 \ldots 100$ km) will significantly alter the early propagation of the flame. For strong off-center ignitions, the buildup time of RT instabilities is shorter corresponding to the larger gravitational acceleration. Still, even for fast-rising blobs, their morphology and, consequently, the effective burning speed will depend critically on small-scale motions of the background (see below).

Despite these advances, the mechanism that leads to a DDT or, alternatively, to a fast deflagration in the nonlinear regime of instabilities is not well understood . Possible candidates for the mechanism are, among others, the Zeldovich mechanism, i.e., mixing of burned and unburned material (Khokhlov, Oran, & Wheeler 1997; Niemeyer & Woosley 1997), crossing shock waves produced in the highly turbulent medium, or shear flows of rising bubbles at low densities (E. Livne 1998, private communication). Currently, none of the proposed mechanisms have been shown to work in the environment of SNe Ia. The Zeldovich mechanism leads to a DDT only if the density and temperature fluctuations remain small (Niemeyer 1999), and the effectiveness of crossing shock waves or shear flows has yet to be demonstrated. However, as a common factor, all these mechanisms depend on the physical conditions prior to the DDT.

From the analysis of light curves and spectra, and the study of flame fronts in SNe Ia, there are strong indications for the importance of the initial structure of the WD prior to the nuclear runaway.

In this work we present the evolution of the WD just prior to the thermonuclear runaway based on multidimensional calculations. In particular, we want to address the following questions:

1. Do mixing processes change the chemical structure of the WD prior to the explosion?
2. Does the thermonuclear runaway occur in multiple spots?
3. Does the thermonuclear runaway happen in a static WD?

In § 2 we present the setup of our calculations. In § 3, the results are presented. In the final, concluding section, we discuss the results in the context of the modeling of SNe Ia, the use of SNe Ia as cosmological yard sticks, and the limits of our study.

2. NUMERICAL METHODS AND SETUP

The initial model has been constructed from results for the stellar progenitor evolution based on the code FRA-

NEC (Straniero 1988; Chieffi & Stranieri 1989; Limogni, Straniero, & Chieffi 2000). The subsequent accretion phase on the WD has been followed up to the thermonuclear runaway by solving the standard equations for stellar evolution in a Henyey scheme (Höflich et al. 2000). Nomoto's equation of state is used (Nomoto 1982). For the energy transport, conduction (Itoh et al. 1983), convection in the mixing length theory, and radiation are taken into account. Radiative opacities for free-free and bound-free transitions are treated in Kramer's approximation and by free electrons. A nuclear network of 35 species up to ^{24}Mg is taken into account based on the reaction network of Thielemann, Nomoto, & Hashimoto (1996).

For our study of multidimensional effects, we start from a WD model several hours before runaway. The spherical model is remapped on a spherical grid with 191 radial and 31 angular (Θ) zones within a cone with Θ between 45° and 135°. The radial resolution has been decreased by a factor of $\approx$10 from the inner to outer layer to properly resolve the central regions. Note that the effective Reynolds numbers are on the order of 30 in the convective region. Thus, we cannot resolve the small-scale turbulent motion, but our study is limited to the large-scale convective flows. The initial structure is relaxed on this grid assuming a pure C/O mixture. To carry out multidimensional simulations of the interior convection and because of the low Mach number of the associated flows, a compressible implicit hydrocode is required. For available explicit, compressible codes for thermonuclear burning, the sound crossing time over a resolution element limits the time step, i.e., CFL condition that imposes hopelessly short time steps. Therefore, for the further evolution, we use an implicit, Eulerian two-dimensional hydrodynamic code (J. Stein, Z. Barkat, & J. C. Wheeler 2002, in preparation). The perpendicular velocity is assumed to be zero (reflective) at all boundaries. The hydrodynamic equations are solved in a second-order scheme including first-order centrifugal and Coriolis forces. Radiation transport effects have been neglected. For the equation of state, we use a relativistic Fermi gas with Coulomb corrections, and radiation. Nuclei are treated as an ideal, nonrelativistic gas without crystallization. For the nuclear burning, analytic expressions have been used for the production of nuclear energy (Rakavy & Shaviv 1968; Barkat et al. 1990), calibrated by an α-network, and tested against the detailed network given above (Thielemann et al. 1996). The time step has been limited by the flow of the material from zone to zone. Typically, the maximum exchange of matter is limited to $\approx$5%. We use standard quadratic artificial viscosity and small second-order Lax-Wendroff Flux throughout the star. Small first-order Lax-Friedrichs Flux is used in the inner three rows of cells and in the outer cells. Small-scale fluctuations were introduced to initialize the convection. Tests showed that the results do no depend on the initial spectrum of the fluctuations.

3. RESULTS

The structure of the initial model of the C/O WD is based on a star with 3 $M_\odot$ at the main sequence and solar metallicity that, at the end of its evolution, has lost all of its H and He-rich layers. By accretion, its core has grown close to the Chandrasekhar limit (Dominguez et al. 1998; Dominguez & Höflich 2000). The temperature, density, and chemical profile at about 1 day before runaway (in one dimension) have been remapped to the two-dimensional grid. At this time, the central density of the WD is 2×10^9 g cm^{-3}. The carbon concentration in the inner layers with 0.348 $M_\odot$ is a result of the central helium burning during the stellar evolution. For the outer layers, the C/O ratio is close to 1. At this time, the nuclear burning timescales are on the order of days, i.e., much longer than the hydrodynamic timescales ($\approx$1 s). Because the WD is almost isothermal, the entropy is increasing with radius. The initial structure is shown in Figure 1 (after relaxation). In the reference model, the further evolution has been followed up all the way to the thermonuclear runaway. The computational domain extends between 65 and 2000 km in the radial direction. For the detailed study of the runaway, we use an extended computational domain down to 13.7 km.

3.1. *Evolution of the Reference Model*

3.1.1. *The Mixing Phase*

The nuclear timescales are long compared to the hydrodynamic timescales up to a few seconds before runaway. Because most of the mixing of abundances happens during this stage of long nuclear timescales (see below), it will be referred to as "mixing phase."

In Figures 2, 3, and 4, snapshots of the evolution are shown for various quantities at 2 hr, 1 hr, 15 minutes, and 5 minutes before the runaway. Nuclear burning of ^{12}C in the central region increases the entropy and temperature. Consequently, the rate of energy production grows with time. The increase of temperature by about 24% in the central regions results in a decrease of the central density by about 4%. Most of the nuclear energy contributes directly to an increase of the entropy. In addition, the nuclear burning drives large-scale convective flows. Typical velocities of the convective flows increase from about 10 km s^{-1} at 2 hr before runaway (BR) to $\approx$50 km s^{-1} at about 5 minutes BR (Fig. 4; see below). The size of the eddies is comparable to the pressure scale height ($\approx$100 km) (see Fig. 2). The lifetime of individual eddies is on the order of 1 revolution for a mass element, leaving little chance to produce a pattern typical for stationary convective layers. The flow is statistically steady on timescales that are short compared to the nuclear evolution timescales up to about 1 hr before the runaway. Eventually, most of the kinetic energy dissipates and contributes to heating. At the time of the explosion, the kinetic energy is small compared to the nuclear energy produced (7.01×10^{45} vs. 2.456×10^{48} ergs). Initially, the convective region is confined by the chemical boundary. Later on, the entropy grows inside by nuclear burning, and a core of almost constant entropy forms. The convection is confined by the steep entropy gradient as a consequence of the steep entropy rise in the outer layers (caused by the flat temperature profile in combination with the rapidly decreasing density, see above). Owing to the increase of the entropy with time, this boundary is gradually moving outward in both mass and radius. Consequently, material of the carbon-rich mantel and the core are mixed. The carbon concentration in the center increases from 24.7% to 35.6% at the time of the runaway, and its size grows from 540 to 730 km (Fig. 5). Owing to the small energy production, hardly any mixing occurs early on, but the rate of mixing and the change of radius (i.e., the contour with C = 45%) grows strongly with time as the nuclear burning increases. No evidence is found for rising blobs that pass the sharp boundary of convective and nonconvective layers and stay there. Blobs that pass the

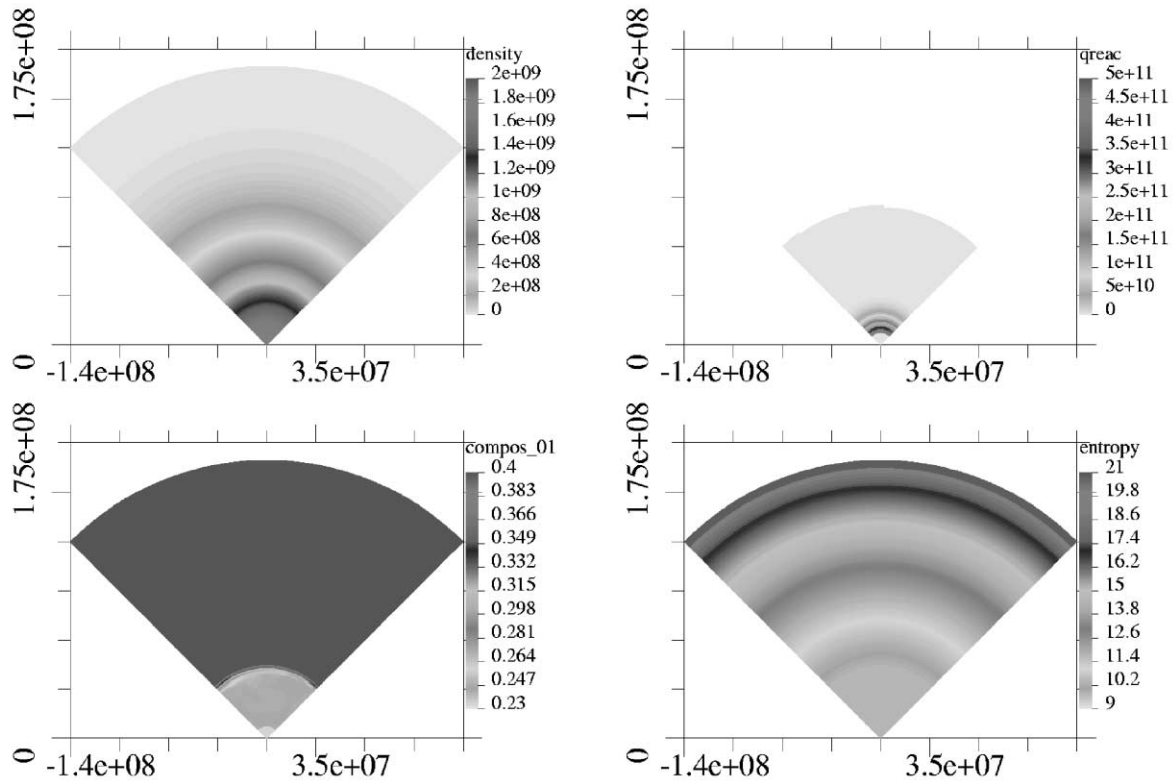

FIG. 1.—Density, carbon concentration, nuclear reaction rate, and entropy (in cgs) are given for the WD with a radius of 1800 km at 3 hr before the runaway for the two-dimensional model, i.e., about 15 minutes after the start of the two-dimensional calculations. Up to this time, the changes in the chemical structures are negligible. The coordinates are given in centimeters relative to the center of the WD. The computational domain in radius and angle is 65–2000 km and 45°–135°, respectively. The horizontal axis is the axis of symmetry. Note that the carbon abundance in the outer layers is 0.5, i.e., outside the color range. [*See the electronic version of the Journal for a color version of this figure*.]

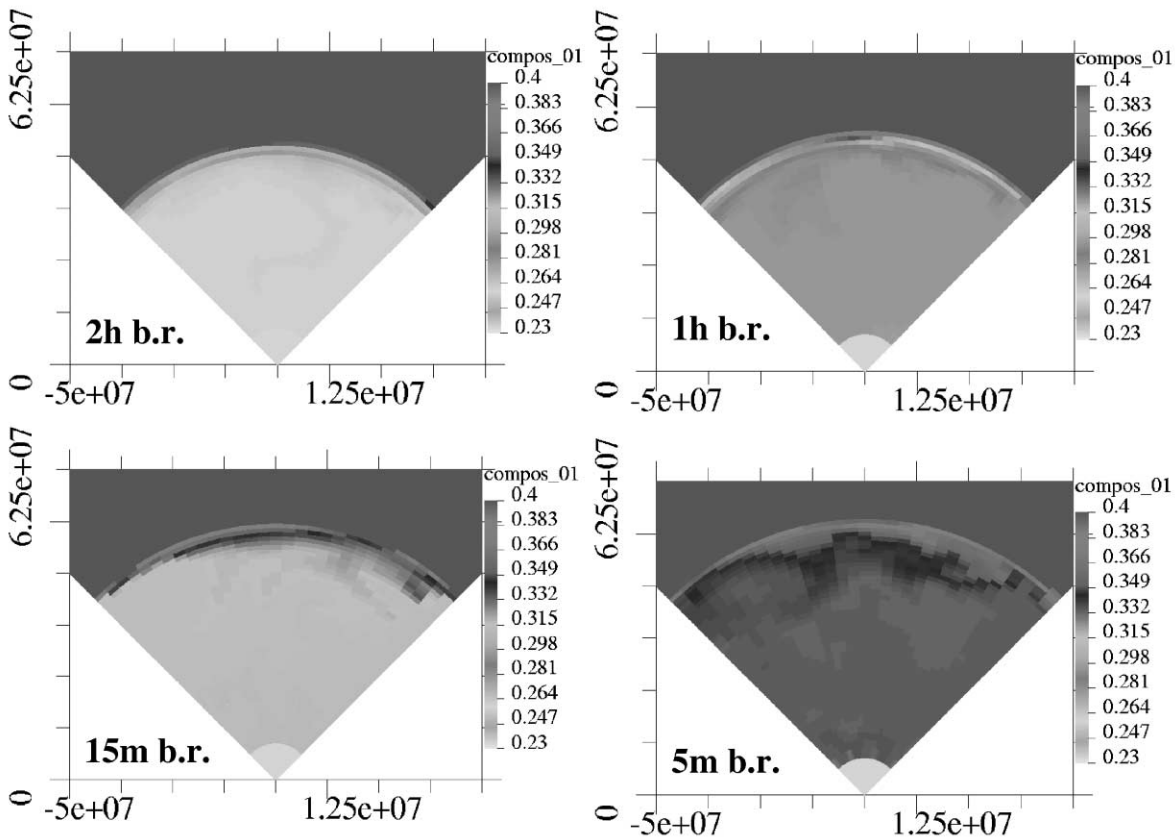

FIG. 2.—Evolution of the structure during the "mixing" phase. Carbon concentration at the inner layers of the WD as a function of time before runaway (BR). The coordinates are given in centimeters relative to the center of the WD. [*See the electronic version of the Journal for a color version of this figure*.]

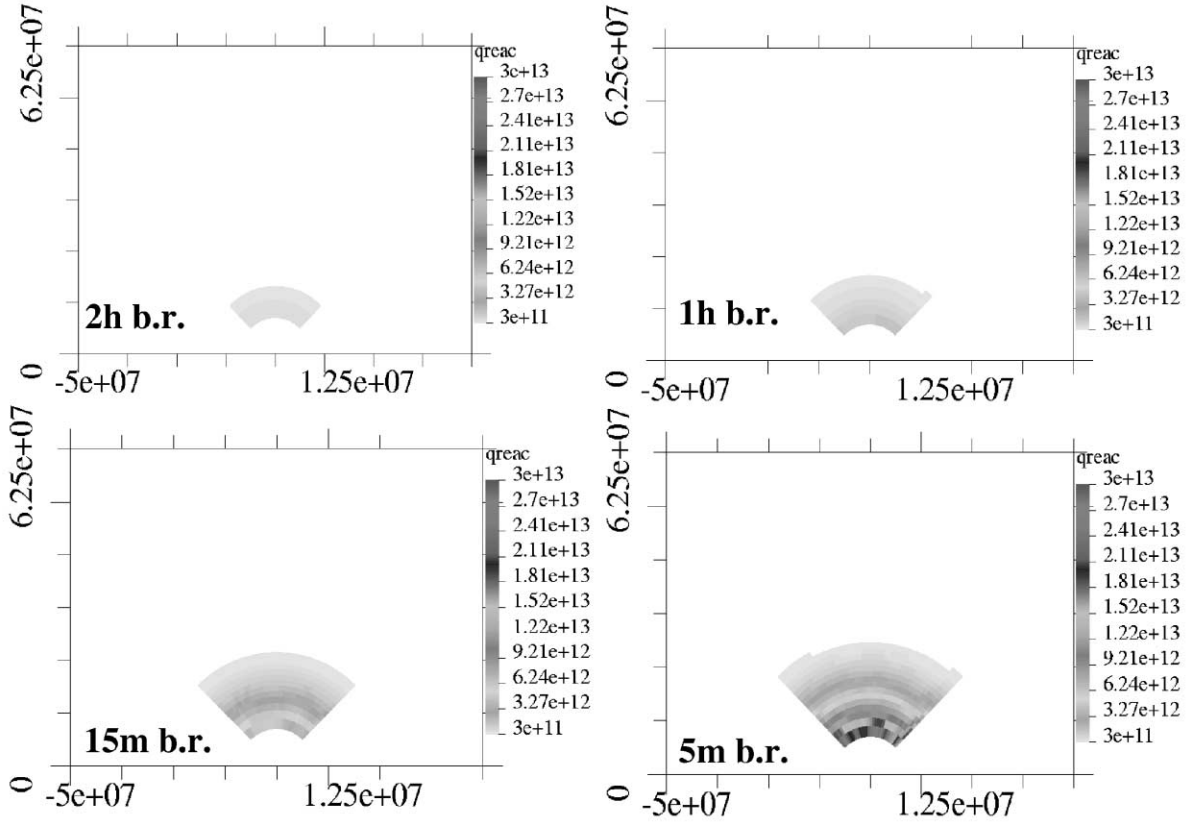

FIG. 3.—Same as Fig. 2, but for the nuclear reaction rates. [*See the electronic version of the Journal for a color version of this figure*.]

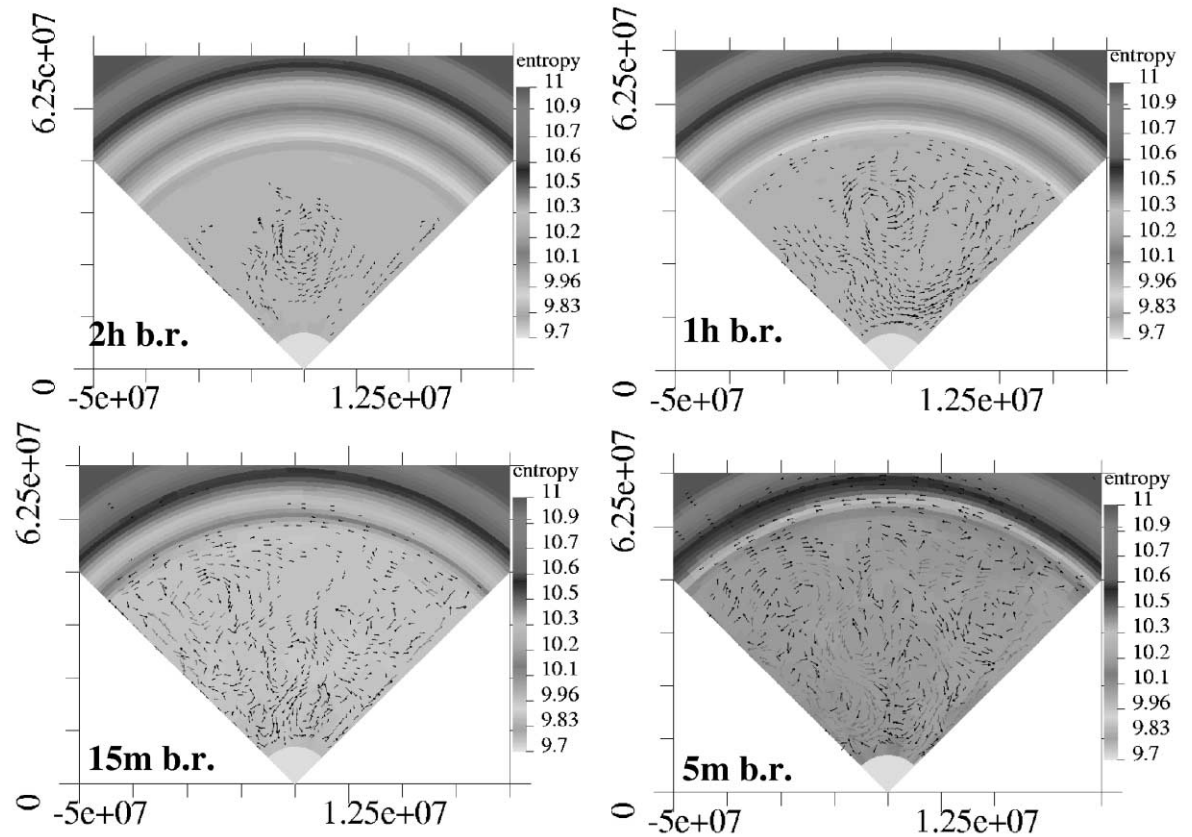

FIG. 4.—Same as Fig. 2, but for the entropy. In addition, the velocity fields are given. Black, red, and green vectors correspond to velocities in the ranges 0–20, 20–40, and 40–60 km s^{-1}, respectively. [*See the electronic version of the Journal for a color version of this figure*.]

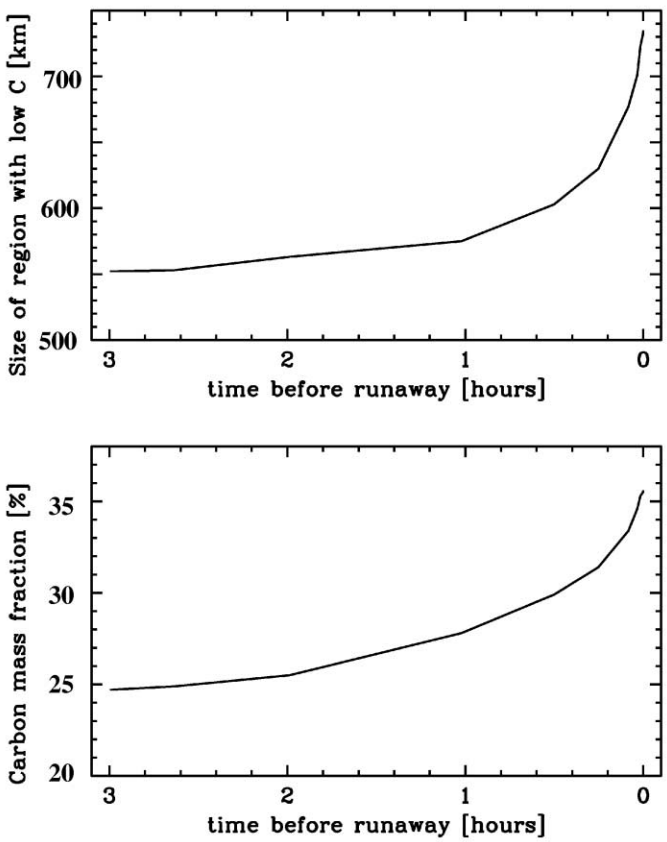

FIG. 5.—Mass fraction and size of the region with low carbon [$X(\mathrm{C}) \leq 45\%$] as a function of time.

boundary tear pieces from the nonconvective layer, creating a new sharp boundary. In stellar evolution, penetration of individual elements of about $0.2H_p$–$0.25H_p$ is assumed by some authors (e.g., Bressan et al. 1993; Schaller et al. 1992). If present, this effect would result in a chemical mixing of the entire WD with timescale of a few hours. In our example, a significant fraction of the WD mass is enclosed within about $3H_p$ above the chemical inhomogeneity which corresponds to a distance of 500 km. If we assume $h = 0.25$ and a velocity of 10 km s^{-1} for the turbulent eddies, the corresponding timescale for complete mixing would be $\approx 3h$.

For any given progenitor structure, the lack of passing blobs through the boundary of convective and nonconvective regions allows us to estimate the total amount of mixing even without detailed calculations. During the phase of slow burning, only a negligible fraction of the carbon is consumed, the turbulent region is confined by the steep entropy gradient at the chemical boundary, and the entropy is almost constant within the turbulent center (Fig. 6). Nuclear runaway occurs in our model when the mean entropy in the core increases to ≈ 10.4. Nuclear burning increases the level of entropy in the core. We can estimate the final amount of mixing and the radius of the core by identifying the distance in the initial model at which the entropy correspond to the critical value for the runaway. Our estimate hardly depends on the exact value of the entropy at the runaway owing to the steepness of the entropy gradients.

3.1.2. *The Nuclear Runaway: The Last 5 Minutes before Runaway*

In Figure 7, we show the final evolution of the temperature and the velocities. Increasing nuclear burning in the

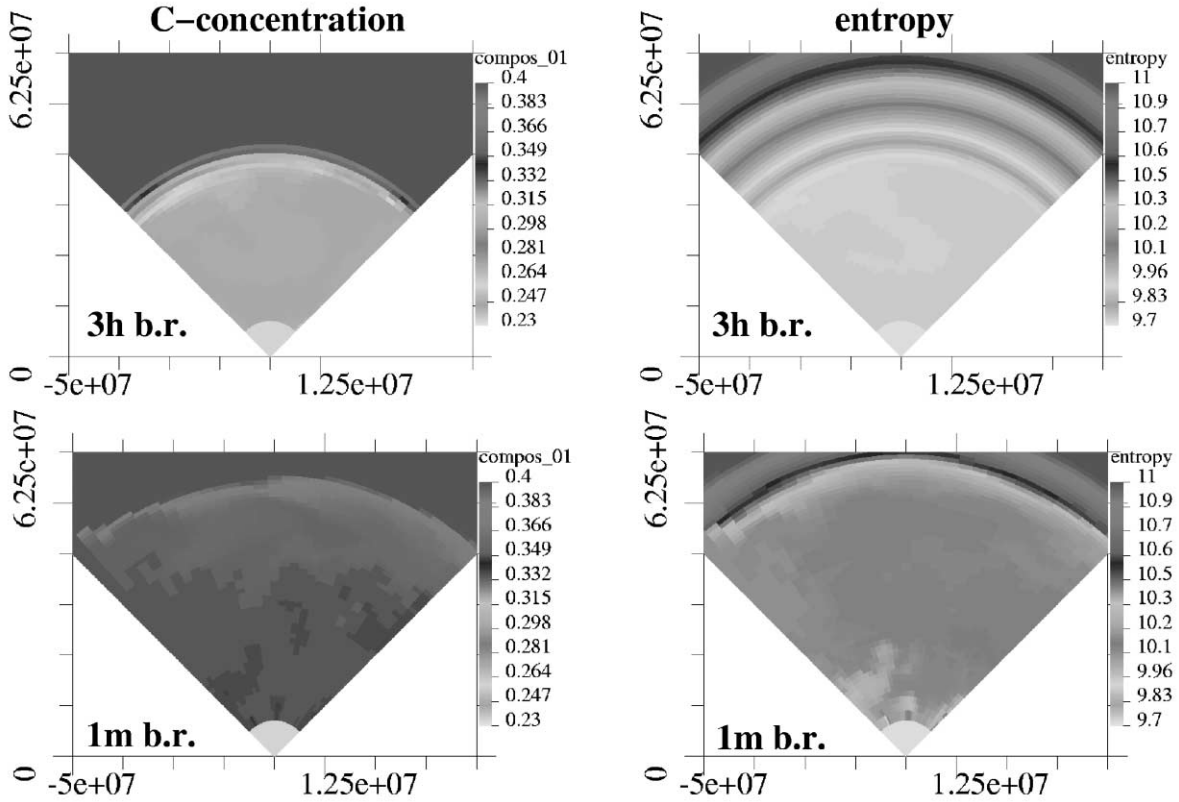

FIG. 6.—Carbon concentration (*left*) and entropy (*right*) at 3 hr (*top*) and 1 minute (*bottom*) before runaway. Runaway occurs when the mean entropy in the turbulent core rises to about 10.1. Note that the final size of the mixed region corresponds to the distance at which the same entropy can be found in the initial model (see text). [*See the electronic version of the Journal for a color version of this figure.*]

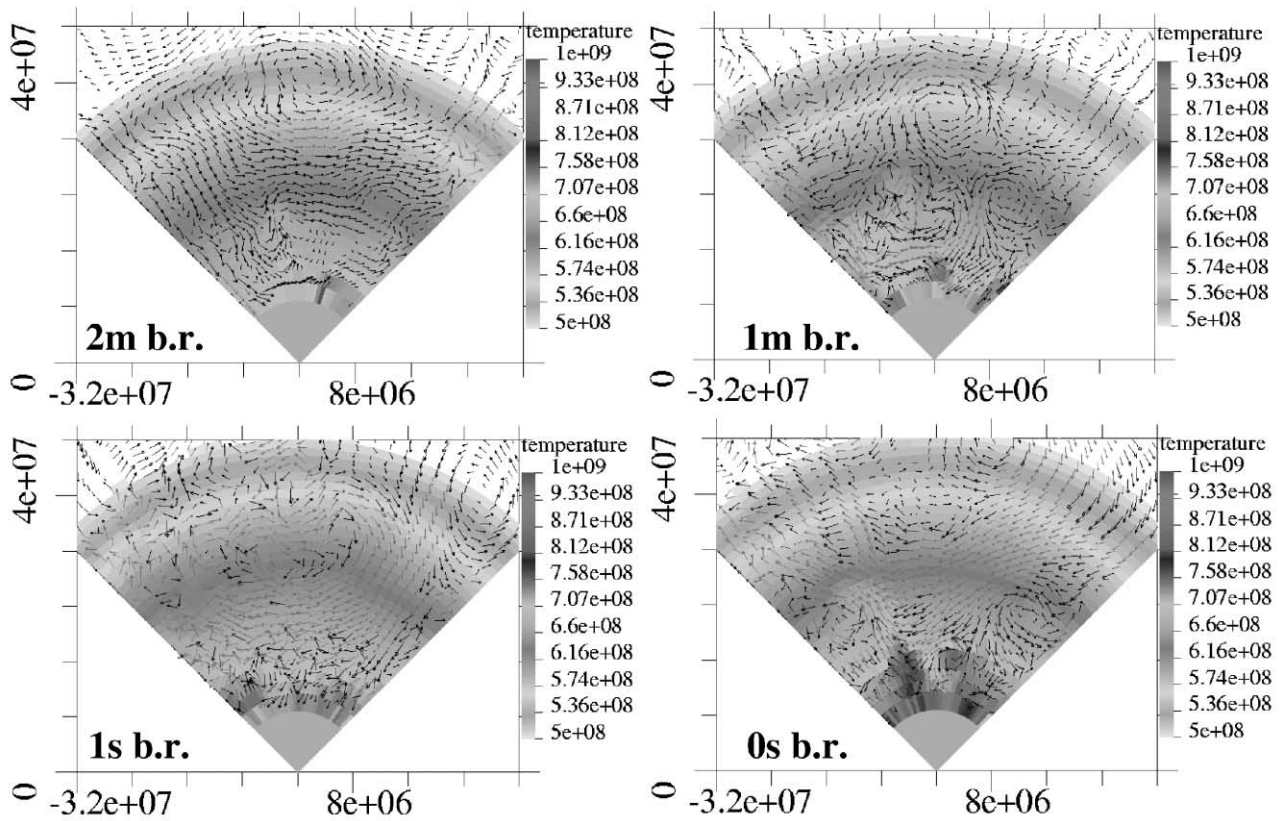

FIG. 7.—Final evolution of the temperature structure up to the runaway. In the lower left plot, the runaway occurs in the second red zone from the left right at the inner boundary ($T = 1.74 \times 10^9$ K). In addition, the velocity field is given. Black, red, and green vectors correspond to velocity ranges of 0–50, 50–100, and 100–150 km s^{-1}, respectively. [*See the electronic version of the Journal for a color version of this figure.*]

inner 100 km drives increasingly strong convection. The region of enhanced energy production heats up material. This hot material starts to rise. Typical turbulent velocities increase from $\approx$50 to $\approx$100 km s^{-1} at the time of the runaway.

The unsteady convective flows are a key factor in understanding the trigger for the final thermodynamic runaway. It explains why we do not see ignition in multiple spots or a strong "off-center" ignition. Owing to convective mixing, the entropy remains nearly constant in all but the very inner layers with a central distance $\lesssim$150 km. There large-scale convective motion brings in material radially. Eventually, compressional heat causes the thermonuclear runaway close to the minimum distance of the corresponding eddy. In the reference model, the thermonuclear runaway occurs very close to the inner boundaries at a distance of 65 km in one specific cell. In general, we do not expect multiple spot ignition because the size of the eddies is larger than the central distance of the point where the runaway occurs. We note that the convection also operates at larger distances from the center, but there the relative changes in radius and, therefore, the release of compressional heat is insufficient to bring material to the point of explosive nuclear burning. We expect that the thermonuclear runaway occurs earlier than in one-dimensional models in which it is triggered by the overall compression of the WD.

To study the thermonuclear runaway in more detail, we have recalculated the final stages up to the runaway for the same model, but the computational region has been extended down to 13.7 km. For computational efficiency, we started with an increased rate of nuclear reactions by factors of 200 down to 4 up to about 10 minutes and 127 s before the explosion, respectively. At 127 s, the resulting structure resembles very closely the reference model for the entropy, the density, and the chemical structure because the main effect of the nuclear burning is an increase of the entropy, the resulting mixing, and the short lifetime of convective cells (see §§ 3.1.1 and 3.1.3). However, the increased heating results in a slight increase of the total kinetic energy at t=127 s by about 10% compared to the reference model. Figure 8 shows the final structure at the onset of the thermonuclear runaway for the inner 120 km. Any deviations from a radial structure are limited to this inner region. Eventually, the thermonuclear runaway occurs in one cell at about a distance of 27 km. During this last phase, the strong release of nuclear energy drives the large scale of violent motion of the matter. The pattern in the temperature and energy release follows the large-scale motion. Most noticeable is the carbon-like pattern of the temperature distribution close to the center (Fig. 8, *lower left panel*). The density shows only very minor deviations from sphericity. At this stage of evolution, carbon is locally depleted by about 1%–2% owing to the nuclear burning, and again it is carried by the velocity field.

We want to discuss the evolution to the thermonuclear runaway in some detail. As shown above, the structure of the entropy, temperature, nuclear energy production, and chemistry can by understood in the same way as a result of the convective motion. As an example, the evolution of the temperature and the velocity field is shown in Figure 9. In the following, the coordinates in brackets provide the coordinates of features in the (x, y) plane in km. At about 3.54 s

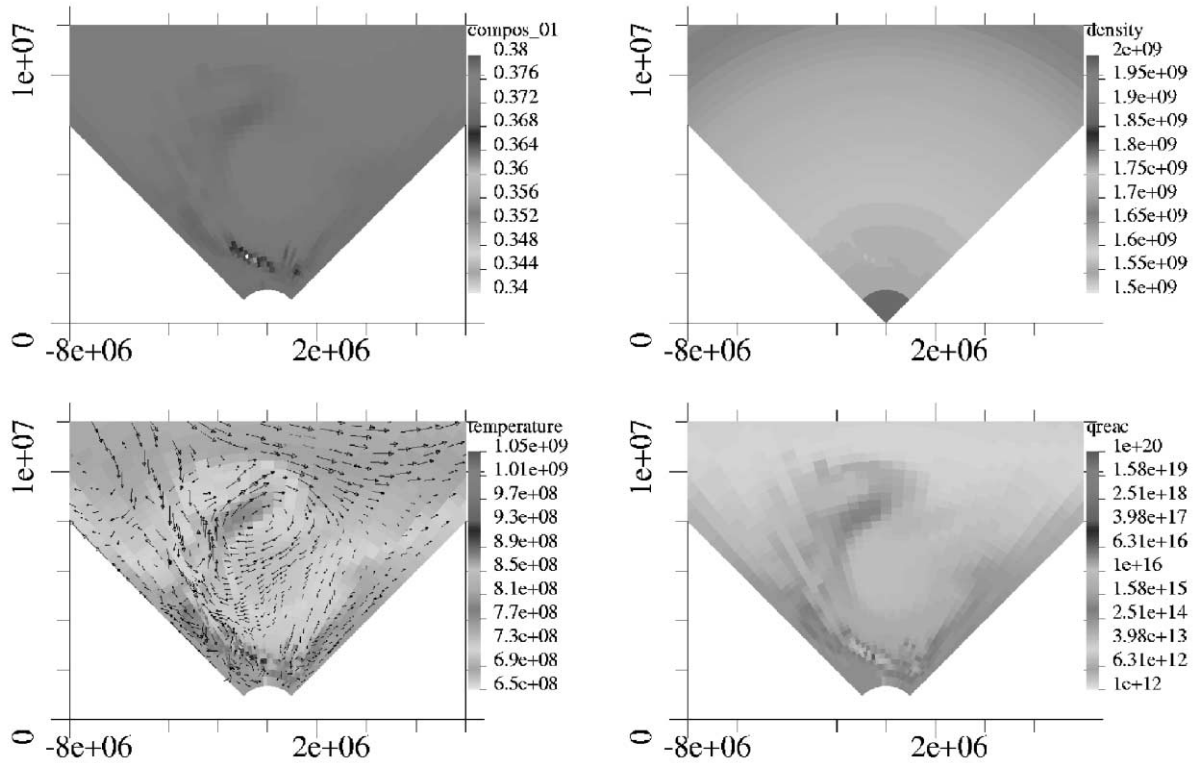

FIG. 8.—Carbon concentration, temperature, nuclear energy generation, and entropy at the runaway for a model with the same physics as the reference model but with a smaller inner "core" of 13.7 km instead of 65 km. In this cell C (and O) has been depleted by the explosive nuclear burning. For computational efficiency, the nuclear rates have been increased up to about 1 minute before the runaway. The runaway occurs in the upper left red cell ($T = 5.14 \times 10^9$ K). The cell has a size of $\approx$2 km, and it is at a central distance of 27 km. The neighboring red cell has a temperature of 1.06×10^9 K, i.e., before runaway. In addition, the velocity field is given. The longest vectors in black, red, and green correspond to velocities of 50, 100, and 150 km s^{-1}, respectively. Typically, the velocities are between 30 and 60 km s^{-1}. [*See the electronic version of the Journal for a color version of this figure*.]

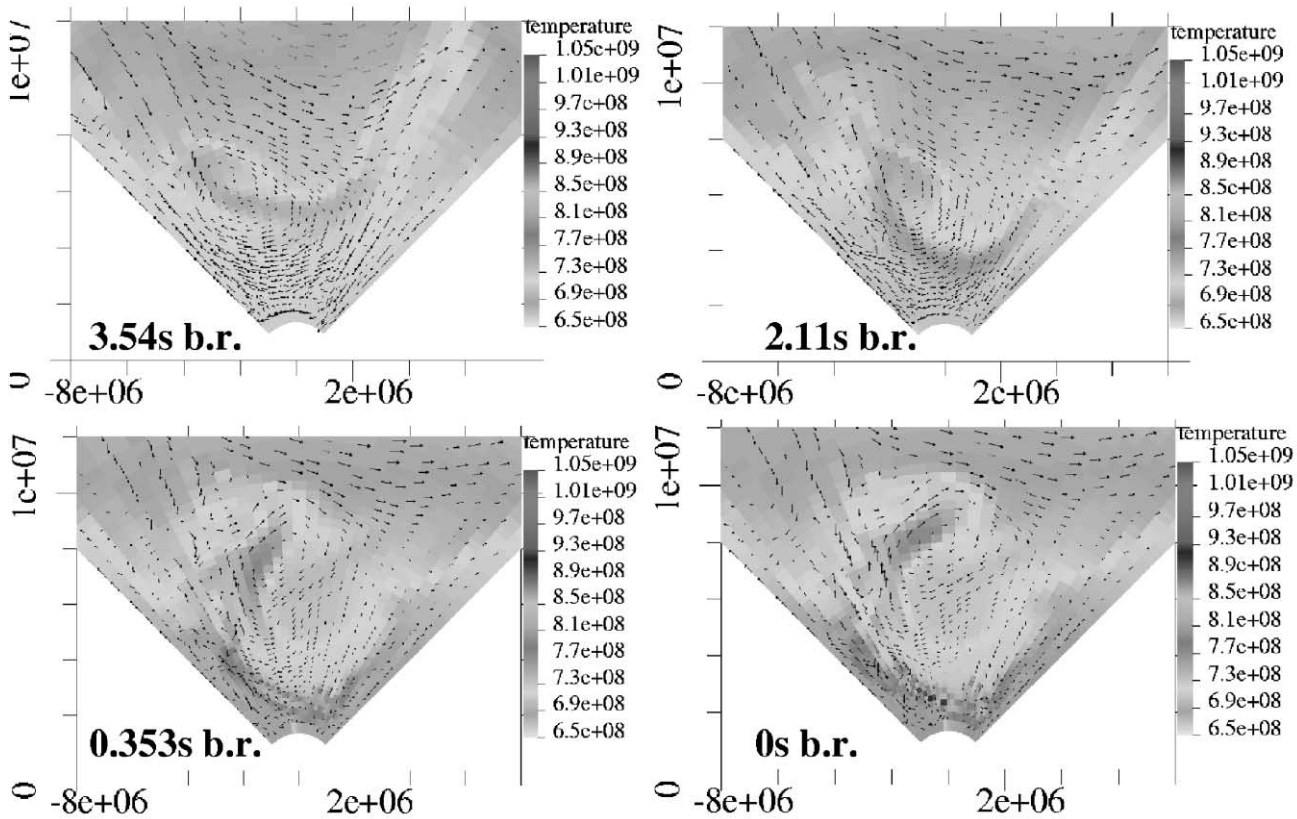

FIG. 9.—Same as Fig. 8, but for the final evolution of the temperature structure up to the runaway for the model with an inner cavity of 13.7 km. [*See the electronic version of the Journal for a color version of this figure*.]

(Fig. 9, *upper left plot*) before the runaway, the temperature structure starts to deviate from the radial structure. The high-velocity field at the upper part of the plot (*red arrows*) is part of a larger vortex A with the center at (150 km, −10 km) that extends down to about 70 km. Close to the center of the WD, nuclear burning drives a convective flow in the opposite direction. These two regions are separated by a layer with higher temperature and low velocities. Owing to the shear, a new, small vortex B is evolving at (−15 km, +65 km). It results in a redirection of the material flow at the lower edge of vortex A. This material flow is directed inward and compresses and heats up material in front of the flow pattern. At about 0.353 s, the temperature has risen up to 8.5×10^8 K. Eventually, further compression and burning cause a rise in temperature up to the onset of explosive carbon burning ($\approx T \geq 1.3 \times 10^9$ K).

Previously, Garcia-Senz & Woosley (1995) studied the details of the thermonuclear runaway in one dimension. They considered plumes rising in a static background. They found that the runaway occurs in rising plumes that rise with velocities of about 5–30 km s^{-1} at central distances of 30 and 100 km s^{-1}, respectively. The runaway occurred when the increase in the thermonuclear burning in the plume becomes stronger than the cooling by expansion. In our simulations, we similarly see that plumes with increased burning tend to rise close to the thermonuclear runaway. In our calculations, these plumes form close to the central region ($\leq 30 \ldots 60$ km) owing to the temperature increase close to the center. At times close to the runaway, the nuclear energy production in the plumes almost compensates for the cooling. However, in a moving background (with velocities $\leq$100 km s^{-1}), the rising plume is disrupted, and parts find themselves in both a rising and descending velocity fields. For those parts that go downward by the current, adiabatic expansion will not avoid the runaway, but, in contrast, compression will push the element over the "edge." In a nonstationary WD, the thermonuclear runaway will occur slightly earlier than in a static WD.

3.1.3. *Effects of the Nuclear Reaction Rates*

We have studied the sensitivity of our results to the assumptions and uncertainties related to the nuclear energy production. In particular, the reaction $^{12}C(\alpha, \gamma)^{16}O$ must be regarded as uncertain by a factor of 3 (e.g., Buchmann 1997) despite some indirect evidence that favors a large cross section. This indirect evidence stems from recent studies of pulsating WDs (Metcalfe, Winget, & Charbonneau 2001) and from the rise times of light curves of SNe Ia (Höflich et al. 1998; Dominguez et al. 2001). Stellar evolution for the asymptotic giant branch favors also a high cross section for $^{12}C(\alpha, \gamma)^{16}O$, but a low value can be compensated for by an increased mixing of helium into the stellar core (e.g., Salaris, Cheffie, & Straniero 1993).

We have scaled the rate for the nuclear energy production by factors f between 1 and 200 (Table 1). For the same initial model, a higher production of nuclear energy drives a faster convection (see E_{kin} in Table 1), and it decreases the time until the thermonuclear runaway; i.e., the nuclear burning timescales are reduced by the factor f. This leaves less time for mixing coupled with increased fluctuations of the central carbon abundance, so a large f implies that a lower compression is required to trigger the explosion. In all calculations, single spot ignition has been found. However, the central distance of the thermonuclear explosion increases from 27 km ($f = 1$) to about 90 km ($f = 200$), and the typical, convective velocities increase slightly. The fluctuations in the carbon concentration rise from the 1% level to about 5%. The amount of carbon mixing decreases with an increasing reaction rate, but, overall, it is rather insensitive for $f \leq 20$ (Fig. 10).

TABLE 1
INFLUENCE OF ENHANCEMENT FACTOR f AT ONSET OF RUNAWAY

Factor f	C (percent)	r(ignition) (km)	E_{kin} (ergs)
+200	26±1	90	...
+50	32.5	86	...
+20	35.5	71	8.5E45
+4	36.2	32	8.2E45
+1	37.0	27	6.9E45

NOTE.—Influence of the enhancement factor f of the nuclear reactions on the distance r(ignition) at which the thermonuclear runaway occurs, on the mean carbon concentration C, and the kinetic energy at the onset of the runaway.

3.2. *Final Discussions and Conclusions*

We have studied the final hours of a Chandrasekhar-mass WD prior to the thermonuclear runaway to investigate the preconditioning of exploding WDs, namely, chemical mixing and the ignition process.

The initial model has been constructed from results of stellar evolution for a star with 3 $M_\odot$ with solar metallicity, followed by a subsequent accretion phase close to the onset of the thermonuclear runaway (Dominguez et al. 2001). The WD has a mass of $\approx$1.37 $M_\odot$. Its chemical structure is characterized by a central region of 0.348 $M_\odot$ with a low carbon concentration ($\approx$24%) surrounded by a mantel with $C/O \approx 1$ originating from the He shell burning and the phase of accretion. A few hours before runaway, the thermal structure of the progenitor shows a rather flat temperature profile and a steep entropy profile because of the rapidly dropping density.

Prior to the runaway, the central regions undergo mild carbon burning. The resulting energy release drives convective motion in the inner region of low carbon concentration and, gradually, increases the entropy of the core up to the point of ignition. Owing to the convection, the entropy of the core is almost constant. Within the resolution of our models, the carbon-concentration gradient at the boundary between the core and the mantle prevents direct mixing, e.g., owing to overshooting convective elements. However, the increasing entropy of the core results in a negative entropy gradient at the core boundary that compensates for the carbon-concentration gradient. This increases the region with constant entropy and produces mixing of carbon-rich region into the core with typical fluctuation of about 1%. We find that the central carbon abundance increases from 24% to about 37%. The initial WD is not homogenized, but the jump in the carbon abundance is reduced by a factor of $\approx$2.

At the time of the explosion, a pattern of large-scale convective elements has been established with sizes of typically 100 km and convective velocities between $\approx$40 and $\approx$120 km

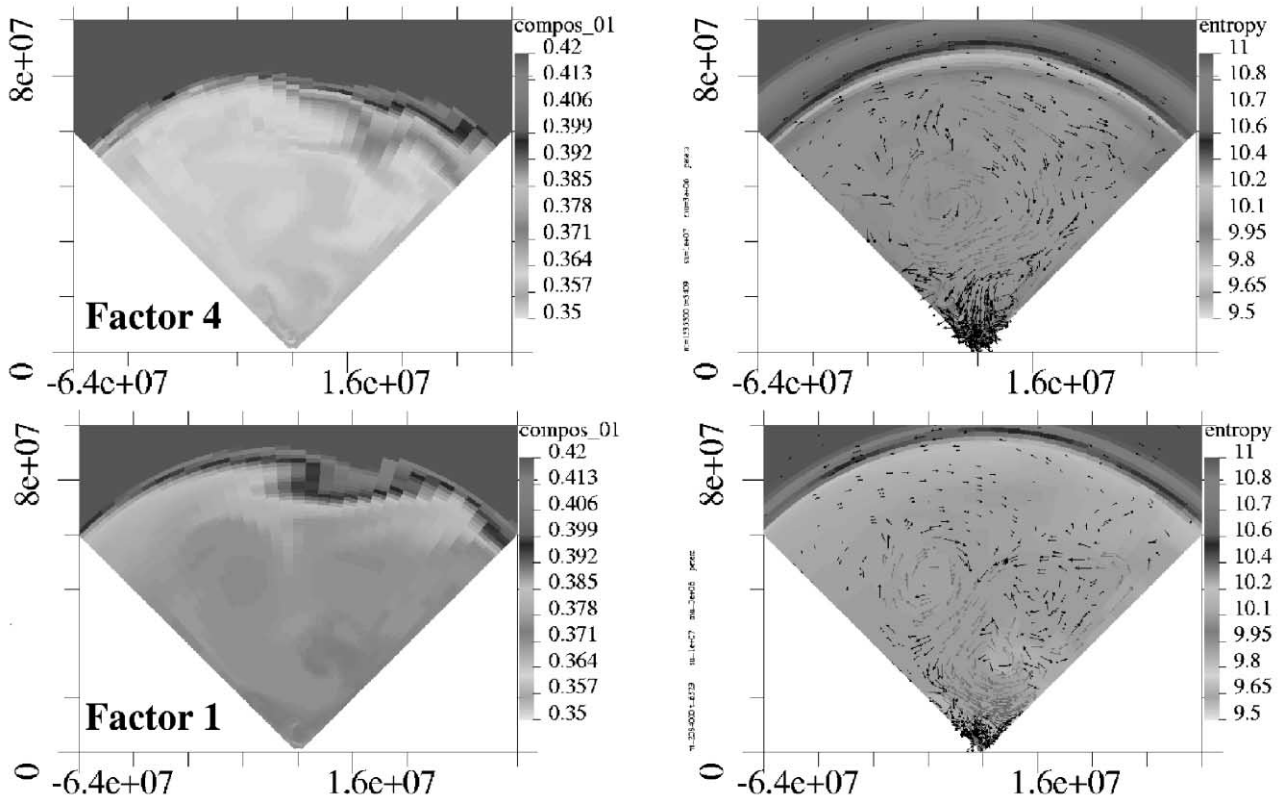

FIG. 10.—Effect of the nuclear reaction rate on carbon abundance and the distance at which the runaway occurs for a nuclear reaction rate increased by a factor of 4 (*top*) compared to 1 (*bottom*). [*See the electronic version of the Journal for a color version of this figure.*]

s^{-1}. Differential velocities between adjoining eddies are larger by a factor of 2, which is well in excess of the laminar deflagration speed. Thus, the change of the morphology of the burning front of SNe Ia is determined by the preconditioning of the WD during the early phase of the explosion for ≈ 0.5–1 s (Dominguez & Höflich 2000; Khokhlov 2002). Niemeyer et al. (1996) found significantly shorter timescales for the growth of RT instabilities in their study of strongly off-center explosions. This can be expected as a result of the larger gravitational acceleration. Still, even for their fast-rising, large-scale blobs ($\approx$1000 km s^{-1}), the morphology of the plumes and, consequently, the effective burning speed will depend critically on small-scale motions of the background. The effective surface of the front will be increased resulting in significantly higher burning speeds. Faster burning implies a larger region of low proton-to-nucleon ratio and, thus, a larger production of neutron-rich isotopes in the central region. On the other hand, a reduction of the timescales for electron capture can be expected, leading to the production of less neutron-rich isotopes. Possible consequences for current estimates on the limits on the central densities of the WD should be noted (Brachwitz et al. 2000).

The explosive nuclear burning front starts in one well-defined region close to the center ($\approx$30 km). The size of the ignition region is determined by the grid resolution ($\approx$2 km). The explosive phase of burning is triggered by compressional heat when matter is brought inward by convection. It starts close to the center because there the adiabatic heating combined with thermonuclear reactions are most effective for a given size of turbulent elements. We find no evidence for multiple spot or strong off-center ignition. We do not expect it because the size of the eddies is comparable to the central distance of the ignition point the lack of and because of any mechanism that would cause a synchronization within typical timescales for the runaway ($\leq$0.1 s). Thus, the probability is fairly small for having a second ignition point during that time.

In the following, we wish to put our basic results into context for our understanding and the quantitative modeling of SNe Ia. As mentioned in the introduction, the propagation of the deflagration front depends on the energy release and, consequently, on the fuel (Khokhlov 2002). We find that the chemical profile in the WD will be strongly changed but in a predictable way. We find that the initial velocity field must be expected to alter the flame propagation during the deflagration phase. Although the actual deflagration speed has little effect on the overall chemical structure of DD models with the exception of the production of neutron-rich isotopes close to the center, all proposed mechanisms for the DDT identify the preconditioning of the material during the deflagration phase as a key element (see § 1), which, in turn, is strongly effected by the initial WD.

We may suspect from the comparison between normal bright and subluminous SNe Ia and the role of the DDT transition for the brightness decline relation that the precondition of the WD may be the "smoking gun" for our understanding of the diversity of SNe Ia.

As mentioned above, the overall chemical structure of the initial WD is preserved, and the turbulent velocity field is limited to the inner, carbon-depleted core. Both the velocity field and the carbon-concentration influence the burning front. Therefore, the mass of the progenitor has a direct influence on the outcome because the core size depends mainly on the $M_{\rm MS}$ mass of the progenitor. The consequen-

ces are obvious with respect to the evolution of the SNe Ia with redshift and their use as a yardstick to measure cosmological parameters and the cosmological equation of state.

Finally, we also have to mention the limitations. This study should not be seen as a final answer but as a starting point to open a new path that eventually may lead to a deeper understanding of the relation between the progenitor and the final thermonuclear explosion.

This work is based on hydrodynamic simulations in two rather than three dimensions. In either case, the convection is driven by entropy gradients over large distances. These large gradients drive large eddies. Convective eddies lose energy in both the true three-dimensional case and in our two-dimensional simulations mostly by exchange with eddies of different size, but the mechanism and rate of energy loss differ between two and three dimensions (see below). Interaction between eddies of different sizes causes exchange of energy toward larger and smaller eddies (Porter & Woodward 1994).

It is well known that for a fully developed turbulence in an incompressible fluid, the direction of the *average* energy flow is from large-scale eddies to smaller ones in three dimensions, and from small-scale eddies to larger ones in two dimensions (Kraichnan 1967; Rose & Sulem 1978; Kraichnan & Montgomery 1980). The viscosity of the fluid becomes most important, and thus the dissipation of kinetic energy is most efficient for the smallest eddies whose Reynolds number is comparably with unity (Laundau & Lifshitz 1989). For incompressible fluids, the dissipation of kinetic energy is very different in two and three dimensions. In the limiting case of vanishing viscosity and incompressible fluids, the dissipation rate in three dimensions remains finite while it approaches zero in two dimensions because of the inverse cascade in the energy flow. The different behavior of the *average* energy flow in two and three dimensions is caused by quadratic invariants globally conserved by the advection term in the hydro equations (see, e.g., Hasegawa 1985 and, more generally, Vazquez-Semadeni 1991). These quantities are *not* conserved in compressible fluids where the difference between two and three dimensions will be of a different kind. Namely, energy can dissipate by acoustic waves and shocks, in addition to the energy dissipation by viscosity. Thus, the interaction of the largest eddies in a finite space and in the case of a compressible fluid is less clear.

In our simulations, the decay timescales of large eddies are on the order of 1 rotation. The real viscosity of astrophysical fluids is much smaller than the numerical viscosity in our simulations. At the same time, large-scale flows (rolls) have a higher inertia in two dimensions than in three. We do not know whether the lifetimes of the true large three-dimensional eddies are larger or smaller than in our simulations, but we argue that the decay times of 1 rotation may be the right order of magnitude. In the following paragraphs, we argue that the main results hold. No detailed simulations for three dimensions are available for the conditions in Chandrasekhar-mass WDs and subsonic convection. However, three-dimensional studies and simulations for convection in other environments suggest dissipation timescales very similar to our results. For incompressible fluids, the dimensional analysis suggests decay timescales on the order of the revolution time in the largest eddies (Landau & Lifshitz 1989). For fully compressible thermal convection in deep atmospheres, Porter & Woodward (2000) extended their two dimensions to three and found similar results in both cases. Recent simulations for the supersonic case and MHD turbulence by Stone, Ostriker, & Gammie (1998) indicate typical timescales for the energy dissipation in molecular clouds of about 0.3–0.8 revolutions for large eddies, i.e., about 1.5 times faster compared to similar, two-dimensional calculations by Ostriker, Gammie, & Stone (1999).

A further restriction is our resolution that is limited to Reynolds numbers of $\approx$ 30–50, i.e., insufficient to follow the cascades to small scales. Obviously, a high-resolution, full three-dimensional study would be desirable. In spite of this, we expect no qualitative change of our basic conclusions concerning the mixing and ignition process.

It is well known that the mixing properties of two- and three-dimensional unsteady flows differ for both scalar and vector "contaminants." In two dimensions, each large eddy is a huge torus carrying a mass that is a large portion of the convection zone, and one or two large eddies carry the hot material from the burning center and spread it over the convective zone. In three dimensions, each large eddy carries much less mass. Nevertheless, even in three dimensions, the number of large eddies should be sufficient for spreading material over the entire convective zone because mixing continues for hours compared to the few seconds it takes a mass element to cross the convection zone. As mentioned in the last section, the amount of mixing can be understood in terms of the nuclear burning that increases the entropy in the central region in both two- and three-dimensional calculations; therefore, we expect a similar amount of mixing in both cases despite the differences in the mixing properties. However, one may expect some change in the size of the fluctuations in the carbon abundance and entropy (see above).

We do not expect a qualitative change in size of the large eddies at the time of runaway and, therefore, in the ignition process, because the presence of large eddies is determined by their production. The motion is continuously driven by nuclear burning at the innermost layers that produces a rise of heated material over about a pressure scale height. This determines the size of the largest eddies that must be expected to be of similar size in both two and three dimensions. Close to the thermonuclear runaway, the circulation times become larger than the nuclear burning timescales. Unless, in three dimensions, the decay times of large eddies are much shorter than a revolution, the largest eddies must be expected to trigger the ignition in a way similar to the two-dimensional case. Therefore, the probability of ignition in more than one well-defined region remains small. Owing to the resolution of our simulation, this region has a size of several kilometers. We cannot say anything about the ignition process on scales of the nuclear burning front.

We have discussed possible implications for the deflagration front on SNe Ia based on previous studies. Obviously, there is a need for consistent calculations of the deflagration front to quantify our estimates on the propagation of the nuclear flames.

Our results are based on a specific progenitor with a main-sequence mass of 3 $M_{\odot}$. Similar studies may be useful for other $M_{\rm MS}$ with larger or smaller cores with low carbon abundances, and different central densities at the time of the explosion. In light of the analysis of the subluminous SN 1999by (see Howell et al. 2001), other effects such as rotation or crystallization should be considered in the future.

We would like to thank Z. Barkat, A. Glasner, A. Khokhlov, E. Livne, J. Scalo, and J. C. Wheeler for helpful discussions and useful comments, and R. Hix for providing the calibration of the analytic energy production rates. J. Stein would like to thank J. C. Wheeler and the colleagues at the Department for Astronomy for the hospitality during his sabbatical in 1995–1996 when this work was started and during subsequent visits in 1997–2000. P. H. would like to thank the colleagues at the Racah Institute in Jerusalem for the hospitality during his visit. This research was supported in part by NASA grant LSTA 98-022 and by the John W. Cox Endowment Fund to the Department of Astronomy at the University of Texas.

REFERENCES

Arnett, D., & Livne, E. 1994, ApJ, 427, 330
Barkat, Z., Livne, E., Swartz, D. A., & Wheeler, J. C. 1990, in Jerusalem Winter School for Theoretical Physics: Supernovae, ed. J. C. Wheeler, T. Piran, & S. Weinberg (Singapore: World Scientific), 141
Brachwitz, F., et al. 2000, ApJ, 536, 934
Bressan, A., Fagotto, F. Bertelli, D., & Chiosi, C. 1993, A&AS, 100, 647
Buchmann, L. 1997, ApJ, 479, L153
Chieffi, A., & Straniero, O. 1989, ApJS, 71, 47
Dominguez, I., & Höflich, P. 2000, ApJ, 528, 854
Dominguez, I., Höflich, P., & Straniero, O. 2001, ApJ, 557, 279
Dominguez, I., Höflich, P., Straniero, O., & Wheeler, J. C. 1998, in Cosmos V, ed. N. Prantzos & S. Harissopulos (Paris: Editions Frontières), 248
Fisher, A., Branch, D., Höflich, P., & Khokhlov, A. 1998, ApJ, 494, 47
Garcia-Senz, D., & Woosley, S. E. 1995, ApJ, 454, 895
Höflich, P., Fesen, R., Gerardy, C. L., & Sakai, S. 2002, ApJ, in press
Harkness, R. 1987, in 13th Texas Symp. on Relativistic Astrophysics (Singapore: World Scientific), 413
Hasegawa, A. 1985, Adv. Phys., 34, 1
Hatano, K., Branch, D., Lentz, E. J., Baron, E., Filippenko, A. V., & Garnavich, P. 2000, ApJ, 543, L49
Höflich, P. 1995, ApJ, 443, 89 (H95)
Höflich, P., Dominik, C. Khokhlov, A., Nomoto, K., Thielemann, F. K., & Wheeler, J. C. 1996a, in Thermonuclear Supernovae, ed. R. Canal et al. (Dordrecht: Kluwer), 659
Höflich, P., & Khokhlov, A. 1996, ApJ, 457, 500
Höflich, P., Khokhlov, A., & Wheeler, J. C. 1995, ApJ, 444, 831 (HKW95)
Höflich, P., Khokhlov, A., Wheeler, J. C., Phillips, M. M., Sunzeff, N. B., & Hamuy, M. 1996b, ApJ, 472, L81
Höflich, P., Nomoto, K., Umeda, H., & Wheeler, J. C. 2000, ApJ, 528, 590
Höflich, P., Wheeler, J. C., & Thielemann, F. K. 1998, ApJ, 495, 617
Howell, A., Höflich, P., Wang, L., & Wheeler, J. C. 2001, ApJ, 556, 302
Hoyle, P., & Fowler, W. A. 1960, ApJ, 132, 565
Iben, I. J., & Tutukov, A. V. 1984, ApJS, 54, 335
Itoh, N., Mitake, S., Iyetomi, H., & Ichimaru, S. 1983, ApJ, 273, 774
Iwamoto, K., Brachwitz, F., Nomoto, K., Kishimoto, N., Umeda, H., Hix, W. R., & Thielemann, F. K. 1999, ApJS, 125, 439
Kenyon, S. J., & Webbink, R. F. 1984, ApJ, 279, 252
Khokhlov, A. 1995, ApJ, 449, 695
———. 1991, A&A, 245, 114
———. 2002, ApJ, Submitted (astro-ph/0008463)
Khokhlov, A., Oran, E. S., & Wheeler, J. C. 1997, ApJ, 478, 678
Kraichnan, R. H. 1967, Phys. Fluids, 10, 1417
Kraichnan, R. H., & Montgomery, D. 1980, Rep. Prog. Phys., 43, 547
Landau, L. D., & Lifshitz, E. M. 1989, Fluid Mechanics (New York: Pergamon)
Lentz, E. J., Baron, E., Branch, D., Hauschildt, P., & Nugent, P. E. 2000, ApJ, 530, L966
Limongi, M., Straniero, O., & Chieffi, A. 2000, ApJS, 129, 625
Lisewski, A. M., Hillebrandt, W., Woosley, S. E., Niemeyer, J., & Kerstein, A. R. 2000, ApJ, 537, 405
Livne, E. 1993, ApJ, 406, L17
Mazzali, P., Nomoto, K., Cappellaro, E., Nakamura, T., Umeda, H., & Iwamoto, K. 2001, ApJ, 547, 988
Metcalfe, T. S., Winget, D. E., & Charbonneau, P. 2001, ApJ, 557, 1021
Niemeyer, J. 1999, ApJ, 523, L57
Niemeyer, J., & Hillebrandt, W. 1995, ApJ, 452, 779
Niemeyer, J., Hillebrandt, W., & Woosley, S. E. 1996, ApJ, 471, 903
Niemeyer, J. C., & Woosley, S. E. 1997, ApJ, 475, 740
Nomoto, K. 1982, ApJ, 253, 798
Nomoto, K., Sugimoto, S., & Neo, S. 1976, Ap&SS, 39, L37
Nugent, P., Baron, E., Hauschildt, P., & Branch, D. 1997, ApJ, 485, 812
Ostriker, E. C., Gammie, C.F., & Stone, J. M. 1999, ApJ, 513, 259
Paczyński, B. 1985, in Cataclysmic Variables and Low-Mass X-Ray Binaries, ed. D. Q. Lamb & J. Patterson (Dordrecht: Reidel), 1
Perlmutter, S., et al. 1999, ApJ, 517, 565
Phillips, M. M., Lira, P., Suntzeff, N. B., Schommer, R. A., Hamuy, M., & Maza, J. 1999, AJ, 118, 1766
Porter, D. H., & Woodward, P. R. 1994, ApJS, 93, 309
———. R. 2000, ApJS, 127, 159
Rakavy, G., & Shaviv, G. 1968, Ap&SS, 1, 347
Reinecke, M., Hillebrandt, W., Niemeyer, J., Klein, R., & Gröbl, A. 1999, A&A, 347, 724
Riess, A., et al. 1999, AJ, 117, 707
Riess, A., Press, W. H., & Kirshner, R. P. 1996, ApJ, 473, 588
Rose, W., & Sulem, P. L. 1978, J. Phys., 39, 441
Salaris, M., Cheffie, A., & Straniero, O. 1993, ApJ, 414, 580
Schaller, G., Shaerer, D., Meynet, G., & Maeder, A. 1992, A&AS, 96, 269
Schmidt, B., et al. 1998, ApJ, 507, 46
Stone, J. M., Ostriker, E. C., & Gammie, C. F. 1998, ApJ, 508, L99
Straniero, O. 1988, A&AS, 76, 157
Sugimoto, D., & Nomoto, K. 1980, Space Sci. Rev., 25, 155
Thielemann, F. K., Nomoto, K., & Hashimoto, M. 1996, ApJ, 460, 408
Umeda, H., & Nomoto, K. 1999, ApJ, 513, 861
Vazquez-Semadeni, E. 1991, Ph.D. thesis, Univ. Texas, Austin
Wheeler, J. C., Höflich, P., Harkness, R. P., & Spyromilio, J. 1998, ApJ, 496, 908
Whelan, J., & Iben, I., Jr. 1973, ApJ, 186, 1007
Woosley, S. E., & Weaver, T. A. 1994, ApJ, 423, 371
Woosley, S. E., Weaver, T. A., & Taam, R. E. 1980, in Type I Supernovae, ed. J. C.Wheeler (Austin: Univ. Texas), 96
Yamaoka, H., Nomoto, K., Shigeyama, T., & Thielemann, F. 1992, ApJ, 393, L55